THE ASTROPHYSICAL JOURNAL, 459:169–174, 1996 March 1

THE BROADBAND ENERGY DISTRIBUTION OF THE MISALIGNED GAMMA-RAY BLAZAR PKS 0521−365

E. PIAN
Space Telescope Science Institute, 3700 San Martin Drive, Baltimore, MD 21218
R. FALOMO
Osservatorio Astronomico di Padova, V. Osservatorio 5, 35122 Padova, Italy
G. GHISELLINI
Ossevatorio Astronomico di Torino, Strada Osservatorio 20, 10025 Pino Torinese, Italy
L. MARASCHI
Dipartimento di Fisica dell'Università di Genova, V. Dodecaneso 33, 16146 Genova, Italy
R. M. SAMBRUNA[1]
NASA/GSFC, Code 666, Greenbelt, MD 20771
R. SCARPA
Dipartimento di Astronomia dell'Università di Padova, V. Osservatorio 5, 35122 Padova, Italy
AND
A. TREVES
Scuola Internazionale Superiore di Studi Avanzati, V. Beirut 2-4, 34014 Trieste, Italy
Received 1994 July 26; accepted 1995 September 7

ABSTRACT

Simultaneous UV and X-ray observations of the blazar PKS 0521−365 are combined with radio, IR, optical, and γ-ray data taken at different epochs to study the overall emission from 10^9 to 10^{23} Hz. The flux distribution declines from the IR to the UV range ($\alpha_{opt-UV} = 1.4 \pm 0.1$), but *hardens* at higher frequencies. The remarkably flat X-ray spectrum (energy index $\alpha_X = 0.68 \pm 0.12$ in the range 0.2–7 keV) suggests a significant contribution by the inverse Compton process in this band. This is supported by the detection of the source in γ-rays by the EGRET experiment. The full radio-to-γ-ray energy distribution is discussed. Various arguments suggest that the jet is not closely aligned with the line of sight ($\theta \sim 30°$), implying that the observed radiation is weakly boosted. This allows a direct estimate of the importance of different sources of photons available for upscattering. We conclude that in this source the synchrotron photons are likely to be the seeds for the inverse Compton process.

Subject headings: galaxies: individual (PKS 0521−365) — galaxies: jets — gamma rays: observations — radiation mechanisms: nonthermal

1. INTRODUCTION

The flat spectrum radio source PKS 0521−365 is strongly polarized (6%, Angel & Stockman 1980), variable (Eggen 1970; Shen, Usher, & Barrett 1972; Ulrich et al. 1984; Edelson 1992; Falomo, Scarpa, & Bersanelli 1994) and exhibits strong emission lines (Scarpa, Falomo, & Pian 1995, and references therein). Its proximity ($z = 0.055$) allows the detection of the host galaxy and of a bright optical jet (Danziger et al. 1979; Cayatte & Sol 1987; Macchetto et al. 1991; Falomo 1994). Thus it cannot be strictly classified neither as a BL Lac object nor as a highly polarized quasar. The term blazar, intended to include essentially all flat spectrum radio sources, is particularly useful for this source.

During the 1992 May 14–June 4 viewing period, the EGRET instrument onboard *GRO* detected the source in γ-rays at a significance level of 4 σ (Lin et al. 1995, and references therein). The discovery of emission at energies greater than 100 MeV supports the blazar nature of PKS 0521−365.

Here we study the broadband energy distribution of the source using simultaneous UV and X-ray observations taken on 1983 November and combining them with radio, millimeter, and simultaneous near-IR–optical data at different epochs and with the more recently measured γ-ray flux. Parts of these data have been already published separately (see next section for references), but the UV and X-ray observations were never jointly studied, while the circumstance of their simultaneity is crucial in modeling the spectral energy distribution.

Several arguments suggest that the emitting jet in this source is not closely aligned with the line of sight and therefore the continuum might not be strongly boosted by relativistic bulk motion. Assuming this, together with direct observation of broad emission lines, allows us to discuss the relative importance of synchrotron and external photons for the production of γ-rays via the inverse Compton (IC) process. The physical and geometrical parameters of the jet are estimated applying an inhomogeneous relativistic jet model which radiates through the synchrotron self-Compton (SSC) process.

2. OBSERVATIONS AND DATA ANALYSIS

Simultaneous observations of the object with *IUE* (1200–3000 Å) and *EXOSAT* (0.2–7 keV) were performed on 1983 November 2 and 30 (see Table 1). During the first *IUE* observation only the SWP camera (1200–1950 Å) was

[1] NRC Research Associate.

TABLE 1

JOURNAL OF OBSERVATIONS[a]

Date	Instrument	Range	Energy Index	F[b] (2650 Å)	F (1700 Å)	F (1 keV)	F (100 MeV)
1979 Oct 6.....	*Einstein*[c] (IPC)	0.2–3.5 keV	$0.58^{+0.35}_{-0.38}$	...	...	1.03 ± 0.17	...
1983 Nov 2.....	*EXOSAT*[d] (LE + ME)	0.2–7 keV	0.52 ± 0.09	...	...	1.47 ± 0.17	...
	IUE (SWP + LWP)	1300–1900 Å	...	...	340 ± 75	...	...
1983 Nov 30.....	*EXOSAT*[d] (LE + ME)	0.2–7 keV	0.68 ± 0.12	...	...	1.78 ± 0.24	...
	IUE (SWP + LWP)	1300–2800 Å	1.1 ± 0.5	610 ± 130	360 ± 70	...	...
1988 Jan 8.....	*IUE* (SWP)	1300–1900 Å	...	...	330 ± 60	...	...
1992 Aug 29.....	*ROSAT*[e] (PSPC)	0.2–2.4 keV	$0.97^{+0.05}_{-0.07}$	...	...	2.06 ± 0.09	...
1992 May/Jun.....	*GRO* (EGRET)	0.1–5 GeV	1.16 ± 0.36	...	...	...	$(1.3 \pm 0.4) \times 10^{-4}$

[a] Errors represent 90% uncertainties.
[b] Fluxes are in μJy.
[c] A power-law fit at free N_H yielded an energy index $\alpha = 1.14^{+2.4}_{-0.9}$ (Worrall & Wilkes 1990).
[d] The reported results are in good agreement with those obtained by Garilli & Maccagni 1990.
[e] 3869 ± 63 net counts for a total exposure of 4845 s.

exposed, whereas on November 30 both SWP and LWP (2000–3000 Å) spectra were recorded. The UV spectra were extracted with the GEX procedure (Urry & Reichert 1988), flux-calibrated after Bohlin et al. (1990; SWP, see Fig. 1) and Cassatella, Lloyd, & Gonzalez-Riestra (1988; LWP). The November 30 spectral fluxes were binned and averaged in intervals of $\sim$100 Å. These data, dereddened with $A_V = 0.2$, were best-fitted with a power-law model ($F_\nu \propto \nu^{-\alpha}$) through a χ^2 minimization procedure. The resulting energy index is reported in Table 1. Here are given also the integrated, averaged, and dereddened broadband fluxes from both observations at the effective wavelengths of 1700 Å (SWP) and 2650 Å (LWP). No significant variability is seen between the SWP fluxes at the two epochs, in conflict with the finding of Edelson et al. (1992) based on a different extraction method and on a spectral fit. We tend to consider, for this faint source (which has also strong line emission), our broadband fluxes more reliable; moreover, we believe the GEX extraction is particularly suitable for these spectra, due to the low S/N. The X-ray data obtained at both epochs with the LE and ME instruments onboard *EXOSAT* were analyzed by Sambruna et al. (1994). No significant flux variations are present between the two epochs. The results of a power-law fit with absorption fixed at the Galactic value, $N_H = 3.37 \times 10^{20}$ cm^{-2} (Elvis, Lockman, & Wilkes 1989), are reported in Table 1.

X-ray data obtained with *Einstein* (1979) and *ROSAT* (1992) were retrieved from the archives and analyzed again under the hypothesis of a simple power law with a fixed column density. The results are also reported in Table 1.

Near-IR–optical spectrophotometry was obtained in 1988 January at ESO (see Falomo et al. 1993). Simultaneously with our IR-optical observation, we recorded an *IUE* spectrum, at a flux level consistent with those of 1983 (see Table 1). On the basis of this agreement, we combined the 1983 November 30 UV–X-ray data and the 1988 January near-IR–optical data to obtain the spectral flux distribution from the near-IR to the X-ray range shown in Figure 2, together with archival *IRAS* data (Impey & Neugebauer 1988). The near-IR and optical data were dereddened and the stellar contribution of the host galaxy, which is rather strong in this object ($\simeq$50%, Pian et al. 1994), was subtracted.

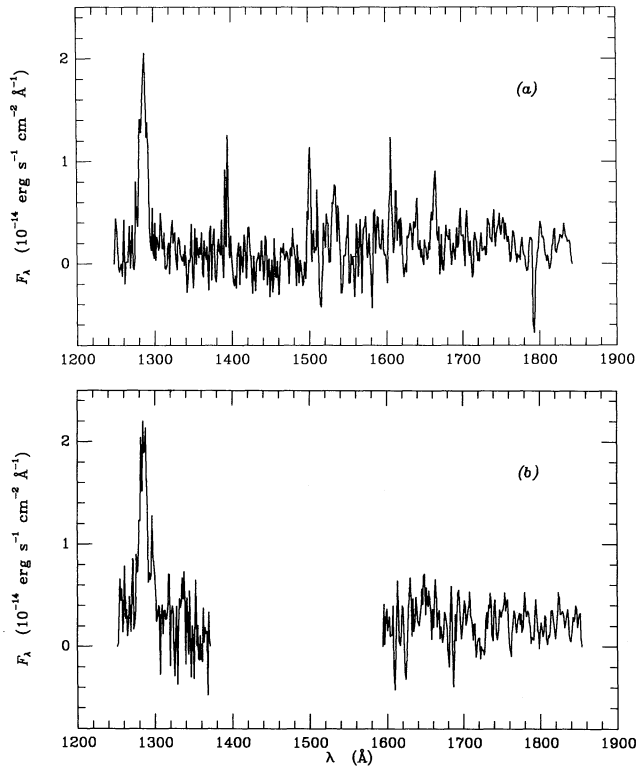

FIG. 1.—*IUE* spectra of PKS 0521−365 taken on (*a*) 1983 November 2 (SWP 21435) and (*b*) 1983 November 30 (SWP 21647).

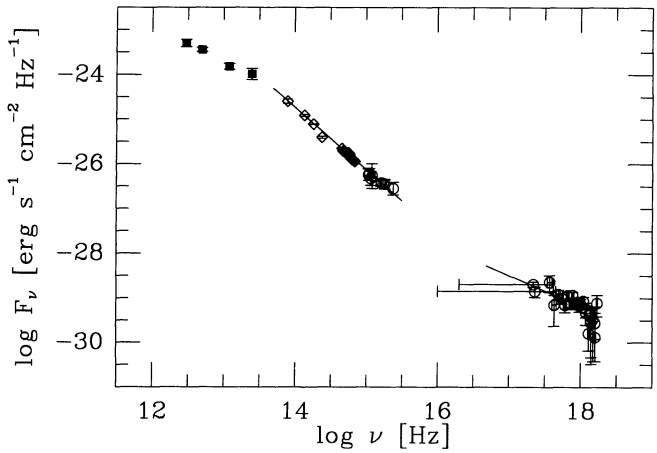

FIG. 2.—Spectral flux distribution of PKS 0521−365 from far-IR to X-rays. Equal symbols are used for simultaneous data. UV and X-ray data (*open dots*) refer to 1983 November 30. Near-IR–optical data (*open diamonds*) refer to 1988 January. Far-IR data (*filled squares*) are taken from the *IRAS* archive. Error bars represent 1 σ uncertainties. The overimposed solid lines represent the power-law best-fit curves to the near-IR-to-UV and to the X-ray data.

It is clear from Figure 2 that the spectral flux distribution steepens around 10^{14} Hz. Above this frequency, the data are consistent with a single power law. A best fit to the combined near-IR, optical, and UV data yields $\alpha = 1.4 \pm 0.1$ at the 90% confidence level ($\chi^2 \simeq 1.3$). An extrapolation of the optical-UV continuum to the X-ray band falls below the simultaneously observed 1 keV flux by almost a factor 10 and the X-ray slope ($\alpha_X = 0.68 \pm 0.12$) is definitely flatter than that in the IR-optical-UV range, suggesting that a different emission mechanism operates in the X-ray band.

3. THE BROADBAND ENERGY DISTRIBUTION

To the near-IR-to-X-ray spectral flux distribution we added the VLBI radio flux measured by Preston et al. (1989); fluxes at millimeter wavelengths (Knapp & Patten 1991); far-IR data from the *IRAS* satellite (Impey & Neugebauer 1988), and the power-law spectral fit determined by Lin et al. (1995) after analysis of the EGRET γ-ray observations ($\alpha_\gamma = 1.16 \pm 0.36$). We thus obtained an overall spectral energy distribution extending over 14.5 decades in frequency. The nonsimultaneity of the far-IR and radio data can clearly affect to some extent the overall spectral shape. At long wavelengths the short- and medium-term variability amplitude is usually not large (see, e.g., Edelson & Malkan 1987; Valtaoja 1994); the yearly variability can be relevant (see, e.g., Grandi et al. 1994), but assuming a maximum flux variation of even a factor of 2, our conclusions do not dramatically change, due to the wide extension of the emitted power range (see § 4.2 and Table 2). On the other hand, as apparent from observations of other blazars, the γ-ray emission can undergo significant variability (see, e.g., Thompson et al. 1994; Maraschi et al. 1994a). The flux used here [$(1.8 \pm 0.5) \times 10^{-7}$ photons s^{-1} cm^{-2} at energy >100 MeV] is the only one reported thus far for this source.

The overall spectral energy distribution is shown in Figure 3 in the νF_ν representation. The X-ray data obtained with *Einstein* and *ROSAT* are also shown in the form of best-fit power laws (absorption was fixed at the Galactic value; see Table 1 for our best-fit parameters). The source intensity at 1 keV varied by a factor 2. The spectral indices derived from *EXOSAT* are consistent with that from *Einstein* (which has rather large errors). The *ROSAT* spectrum is softer than measured either with *EXOSAT* or *Einstein*. This could be due to spectral variability of the source, ($\Delta\alpha \simeq 0.3$ is not uncommon for blazars; see, e.g., Sambruna et al. 1994), but it may also be related to the softer range of the *ROSAT* instrument (Table 1). In fact, an extension of the steep UV component to the soft X-ray band is not unlikely. A similar situation was found in the case of the BL Lac object PKS 0537−441 (Treves et al. 1993).

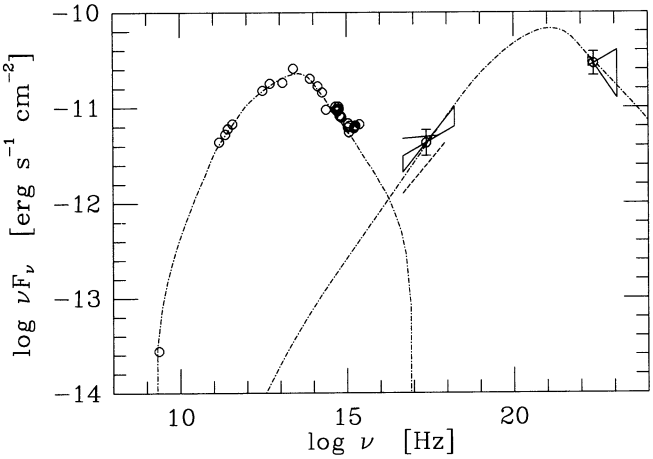

FIG. 3.—Spectral energy distribution of PKS 0521−365. *IUE* and *EXOSAT* data refer to 1983 November 30. The *EXOSAT* power-law spectral fit is reported along with the 1.6 σ (90%) confidence range. For comparison, the power laws representing the *ROSAT* spectrum best fit (*solid line*) and the *Einstein* best fit (*dashed line*) are reported. The 1 σ confidence range of the spectral fit to the γ-ray data as determined by Lin et al. (1995) is also shown. The dashed-dotted line represents the synchrotron and self-Compton contributions within the adopted jet model. Error bars on the low-frequency data points are omitted.

The broadband energy distribution clearly shows two spectral regions where the observed energy output is maximum (see Fig. 3). One component peaks in the far-IR ($\simeq 10^{13}$–10^{14} Hz), the other component shows up between 1 keV and 100 MeV, and probably peaks at energies lower than 100 MeV, as suggested by the γ-ray energy index. In any case, we note that the power in the observed γ-ray band is already comparable to the bolometric power at all other frequencies. The two components apparently join in the extreme UV–soft X-ray range. This "double-humped" energy distribution is similar to that of other blazars (see, e.g., Maraschi, Ghisellini, & Celotti 1994b).

4. THEORETICAL CONSIDERATIONS

4.1. *General Remarks*

It is natural to interpret the double-humped energy distribution of blazars as due to synchrotron and IC emission. The first mechanism can account for the self-absorbed radio emission and for the millimeter, far- and near-IR, optical, and UV continuum of PKS 0521−365, assuming a suitably

TABLE 2

INPUT PARAMETERS FOR AN INHOMOGENEOUS JET MODEL[a]

Parameter	Paraboloid	Cone	1.6 σ (90%) Uncertainty
Spectral index α_0	0.5	0.5	0.1
Magnetic field power-law index m	1	1	0.3
Electron density power-law index n	0.5	1.5	0.1
Maximum frequency power-law index η	1	1	0.3
Emission region profile ϵ	0.5	1	
Inner radius R_0 (cm)	10^{15}	$10^3 R_0$	$0.1R_0$
Outer radius	$10^3 R_0$	$10^5 R_0$	
Initial Magnetic field B_0 (G)	20	0.02	$0.1B_0$
Initial electron density K_0 (cm^{-3})	7.5×10^4	2.4×10^3	$0.15K_0$
Initial maximum synch. frequency ν^s_{max} (Hz)	6×10^{16}	6×10^{13}	$0.25\nu^s_{max}$
Bulk Lorentz factor Γ	1.2	1.2	0.1

[a] Symbols for the relevant parameters are those adopted in Ghisellini et al. 1985.

curved spectral shape of the relativistic electrons or an inhomogeneous jet (see below).

The high-energy emission (X- and γ-rays) can then be produced via IC scattering of the relativistic (synchrotron-emitting) electrons off photons produced in the same region (in this case the high-energy emission is SSC, see, e.g., Maraschi, Ghisellini, & Celotti 1992), or alternatively off photons emitted by an accretion disk (e.g., Dermer & Schlickeiser 1993) or the broad-line region, and/or scattered by some surrounding material (e.g., Sikora, Begelman, & Rees 1993, 1994).

In order to account for the high "apparent" radiation density observed in many objects, it is necessary to assume that the emitting plasma is moving relativistically so that the observed radiation is amplified by relativistic beaming. The case of PKS 0521−365 is of special interest in that the evidence suggests that relativistic boosting *is not large* in this source:

1. The ratio, R_c, of the core to extended radio flux is believed to be a beaming indicator, since the emission from the core is supposed to be beamed, while the emission from the extended components is isotropic (see, e.g., Orr & Browne 1982). The distribution of R_c for BL Lac objects and flat radio spectrum quasars is in the range 1–1000, while the range for radio galaxies (F-R I and F-R II) is 10^{-3} to 1 (see, e.g., Maraschi & Rovetti 1994), supporting unification schemes in which BL Lac objects and flat radio spectrum quasars are F-R I and F-R II radio galaxies observed at small angles (Blandford & Rees 1978; Urry & Shafer 1984; Ghisellini et al. 1993). The value observed for PKS 0521−365, at 1.4 GHz, is $R_c \sim 0.3$ (Antonucci & Ulvestad 1985). Such a small value suggests a modest beaming of the core radio emission in the line of sight direction, and therefore a relatively large viewing angle.

2. Applying the SSC model to the VLBI core of this source (requiring that the radio core does not overproduce the X-ray emission), Ghisellini et al. (1993) found $\delta \sim 1$ for the radio emission.

3. Requiring the source to be transparent to 1 GeV γ-rays, estimating the size from variability, and assuming that the X-rays (which are targets of the γ-rays for the photon-photon process) are cospatial with the γ-rays, Dondi & Ghisellini (1995) found $\delta \sim 1.3$ for the high-energy emission.

Another suggestion of a large viewing angle comes from the presence, in PKS 0521−365, of a well-defined optical jet, with an angular size of 6".5 (7 kpc, Keel 1986; Macchetto et al. 1991; Sparks, Biretta, & Macchetto 1994) and well-aligned with the nucleus. It is a weaker evidence because a well-defined optical jet is visible also in 3C 273, for which other beaming indicators suggest instead a small angle of view. Note, however, that in 3C 273 the VLBI jet is misaligned with the optical jet by an angle of $\sim 20°$ (Unwin et al. 1985). Moreover, unlike the case of 3C 273, no superluminal motion was detected in PKS 0521−365 through VLBI techniques, which further suggests a large viewing angle for the radio jet of the latter source.

Note that a Doppler boosting factor $\delta \sim 1$ means that we are measuring the *intrinsic* continuum of this object.

We can estimate the relative importance of different sources of photons for IC scattering by relativistic electrons in the jet. Approximating the emission region within the jet as a sphere of radius $R_{\rm blob}$ moving with bulk Lorentz factor Γ at an angle θ with the line of sight and defining the Doppler factor $\delta = [\Gamma - (\Gamma^2 - 1)^{1/2} \cos\theta]^{-1}$, the intrinsic (primed) energy density of the internally produced radiation is

$$U'_{\rm int} = \frac{L_{\rm syn}}{4\pi R_{\rm blob}^2 c \delta^4} = 2.6 \frac{L_{\rm syn,44}}{\delta^4 R_{\rm blob,16}^2} \text{ ergs cm}^{-3} \quad (1)$$

since the *observed* synchrotron luminosity $L_{\rm syn}$ corresponds to an intrinsically emitted luminosity $L'_{\rm syn} = \delta^{-4} L_{\rm syn}$. Here $L_{\rm syn,44}$ and $R_{\rm blob,16}$ are in units of 10^{44} ergs s^{-1} and 10^{16} cm, respectively.

From the luminosity in the broad lines $L_{\rm BLR}$ (which is of the order of 6×10^{42} ergs s^{-1}, Scarpa et al. 1995) we can evaluate the energy density of the external radiation, in the rest frame of the blob, where it is enhanced by a factor Γ^2. Assuming a spherical broad-line region with radius $R_{\rm BLR}$, we have

$$U'_{\rm BLR} \sim \frac{L_{\rm BLR}\Gamma^2}{4\pi R_{\rm BLR}^2 c} \frac{(1+\beta)^3}{3\beta} \sim 7.1 \times 10^{-4} \frac{L_{\rm BLR,42}\Gamma^2}{R_{\rm BLR,17}^2} \text{ ergs cm}^{-3}, \quad (2)$$

where $L_{\rm BLR,42}$ and $R_{\rm BLR,17}$ are in units of 10^{42} ergs s^{-1} and 10^{17} cm, respectively.

Another contribution to the radiation energy density may come from photons emitted directly by a disk (see far-UV points in Fig. 3). This contribution is very important close to the disk, but decreases rapidly for larger distance. Assuming that a luminosity L_d is emitted by the inner accretion disk, within a radius R_d, we have

$$U'_d \sim \frac{L_d\Gamma^2}{3\pi\beta c R_d^2} \left\{ \left[1 - \beta \left(1 + \frac{R_d^2}{R_\gamma^2} \right)^{-1/2} \right]^3 - [1-\beta]^3 \right\} \sim 3.5 \times 10^2 \frac{L_{d,44}\Gamma^2}{\beta R_{d,15}^2} \left\{ \left[1 - \beta \left(1 + \frac{R_d^2}{R_\gamma^2} \right)^{-1/2} \right]^3 - [1-\beta]^3 \right\} \text{ ergs cm}^{-3}, \quad (3)$$

where R_γ is the distance of the emitting blob to the accretion disk.

We can see that if δ is of order unity and $\Gamma \lesssim 10$, the external radiation density is unlikely to dominate. In this case, assuming a blob radius $R_{\rm blob} = 10^{16}$ cm, and deriving from the overall energy distribution (Fig. 3) $L_{\rm syn} \simeq 10^{44}$ ergs s^{-1} and $L_d < 7 \times 10^{43}$ ergs s^{-1}, we have that the internal radiation energy density always dominates the contribution from the broad-line region, and dominates the radiation energy density produced directly by the accretion disk if $R_\gamma > 3 \times 10^{15}$ cm.

As a consequence, equations (1)–(3) suggest that the main mechanism for the production of γ-rays is SSC, unless Γ is uncommonly large or the size of the blob is of the same order as the size of the broad-line region. In this respect, note that in the case of a relativistic jet, $R_{\rm blob}$ should correspond to the cross-sectional radius of the jet.

4.2. *Inhomogeneous Jet Model*

In order to be more quantitative, we apply specifically the inhomogeneous jet model of Ghisellini, Maraschi, & Treves (1985) and Ghisellini & Maraschi (1989), where the emitting region is made up of a paraboloid ending up in a cone. The

plasma flow is relativistic, possibly accelerating in the parabolic part of the jet and the electron density and magnetic field are simple functions (power laws) of the radial distance. In this model the overall spectrum is the sum of the local contributions which have different spectra. Energetically, the dominant emission region is the outer part of the paraboloid, which radiates at 10^{13}–10^{14} Hz by synchrotron and in γ-rays by self-Compton, while the conical region is necessary to account for the radio emission.

Although the model is rather simplified, it contains a large number of free parameters. We therefore searched for a solution which appears consistent with the data rather than for a best-fit to the data. The result is shown in Figure 3 and the corresponding parameters are given in Table 2. To take into account the effect of possible variability on the overall spectral energy distribution, due to the nonsimultaneity of the data, we considered the fluxes in the various energy bands as independent and added in quadrature to each flux intrinsic error a frequency-dependent percentage variability estimate (from 5% for the radio up to 90% for the γ-rays, based on typical multifrequency long-term variability of blazars) and consequently determined the 90% probability range for each fitted parameter through a χ^2 routine. This reasonable assumption on the unpredictable occurrence of flux variability allows to assign conservative uncertainties to the computed physical quantities (last column of Table 2).

The model reproduces rather well the data from radio to γ-rays. In particular, it fits well to the slopes of the *EXOSAT* and the *Einstein* X-ray data and to the slope of the EGRET γ-ray data, and accounts for the X-ray and γ-ray fluxes within the uncertainties. Note that in the soft X-ray band the synchrotron and the self-Compton contributions, which have very different spectra, overlap. Therefore, a relatively small relative flux variation may yield a significant spectral variation, which may account for the softer *ROSAT* spectrum. A similar behavior was found in the case of the radio bright BL Lac object PKS 0537−441 (Treves et al. 1993).

In this model, X-rays are coming from SSC scattering of relativistic electrons off the radio and millimeter photons, while the GeV γ-ray emission is produced by SSC off optical-UV photons. This allows to predict a spectral slope for the γ-ray spectrum of $\simeq 1.3$, consistent with the value determined by Lin et al. (1995; $\alpha_\gamma = 1.16 \pm 0.36$).

The observed peak at $\sim 3 \times 10^{13}$ Hz corresponds to the thin synchrotron emission of the intermediate region of the jet (outer paraboloid). The same region is responsible for the self-Compton peak in the MeV band.

The bulk Lorentz factor of the plasma in the paraboloid is constant, $\Gamma \simeq 1.2$ (see Table 2), and the viewing angle is $\theta \simeq 30°$ (with an uncertainty of $\sim 20\%$), implying a Doppler beaming factor $\delta \sim 1.5$ and an apparent plasma velocity lower than the light speed ($\beta_{app} \simeq 0.5$). The small value of the beaming factor is in agreement with the other independent estimates discussed in § 4.1. The presence of only marginally relativistic conditions and of modest beaming is consistent with the observation of the radio and optical jet, which would not be visible if it were strictly aligned with the line of sight; with the absence of observed superluminal motion, and with the modest value of the core dominance parameter.

5. DISCUSSION AND CONCLUSIONS

PKS 0521−365 is one of the three relatively nearby sources detected by EGRET (the other two objects with $z < 0.1$ are Mrk 421 and PKS 2005−489; see Von Montigny et al. 1995). The proximity of these objects allows their detection above 100 MeV even if their γ-ray luminosity does not largely dominate their power output, and even if the entire radiation is not greatly Doppler-boosted. It may be that the dominance of the γ-ray luminosity in other blazars observed by EGRET so far is the result of a selection effect, due to the limited EGRET sensitivity which prevents detection of far-away objects unless they are in "exceptional" flaring state in γ-rays.

The proximity of PKS 0521−365 allows in principle its detectability at TeV energies, like Mrk 421 (Punch et al. 1992) and Mrk 501 (Quinn et al. 1995), since photon-photon interactions with the IR background radiation should be modest (Stecker, de Jager, & Salamon 1992; de Jager, Stecker, & Salamon 1994). However, in our model, the IC component at TeV energies falls much below the threshold sensitivity of present detectors, so that the actual detection is not expected, unless the object undergoes an extraordinarily large γ-ray outburst.

We have shown that the origin of the high-energy emission in PKS 0521−365 is likely SSC process, rather than IC on externally produced radiation. This result is based on the small value of the beaming factor, resulting in a large intrinsic (and internally produced) synchrotron energy density.

The similar output in synchrotron and self-Compton luminosities thus indicates an approximate equipartition between the magnetic and synchrotron energy density in the relativistic jet. This, of course, does not exclude the possibility that in other sources the dominant cooling mechanism is IC on external radiation, as proposed by Sikora et al. (1994).

If SSC is the dominant cooling mechanism in PKS 0521−365, then we can predict a general pattern of variability at different frequencies (see also Maraschi et al. 1994a, b). Assume in fact that the variation in flux is produced by a variation in the density of the relativistic electrons N. Then the synchrotron luminosity varies linearly with N, while the self-Compton flux should be proportional to N^2. If, instead, external radiation is important for the IC mechanism, then both the synchrotron and the Compton components are proportional to N, and should thus vary with similar amplitudes.

We are grateful to H. C. Thomas for providing information on *ROSAT* data in advance of publication, and to O. C. de Jager for his helpful criticism and suggestions.

REFERENCES

Angel, J. R. P., & Stockman, H. S. 1980, ARA&A, 18, 321
Antonucci, R. R. J., & Ulvestad, J. S. 1985, ApJ, 294, 158
Blandford, R. D., & Rees, M. J. 1978, in Pittsburgh Conference on BL Lac Objects, ed. A. M. Wolfe (Pittsburg: Univ. of Pittsburgh), 328
Bohlin, R., Harris, A. W., Holm, A. V., & Gry, C. 1990, ApJS, 73, 413
Cassatella, A., Lloyd, C., & Gonzalez-Riestra, R. 1988, ESA *IUE* Newsletter, 31, 13
Cayatte, V., & Sol, H. 1987, A&A, 171, 25
Danziger, I. J., Fosbury, R. A. E., Goss, W. M., & Ekers, R. D. 1979, MNRAS, 188, 415

de Jager, O. C., Stecker, F. W., & Salamon, M. H. 1994, Nature, 369, 294
Dermer, C. D., & Schlickeiser, R. 1993, ApJ, 416, 458
Dondi, L., & Ghisellini, G. 1995, MNRAS, 273, 583
Edelson, R. A. 1992, ApJ, 401, 516
Edelson, R. A., & Malkan, M. A. 1987, ApJ, 323, 516
Edelson, R. A., Pike, G. F., Saken, J. M., Kinney, A., & Shull, J. M. 1992, ApJS, 83, 1
Eggen, O. J. 1970, ApJ, 159, L95
Elvis, M., Lockman, F. J., & Wilkes, B. J. 1989, AJ, 97, 777
Falomo, R. 1994, ESO Messenger, No. 77, 49
Falomo, R., Bersanelli, M., Bouchet, P., & Tanzi, E. G. 1993, AJ, 106, 11
Falomo, R., Scarpa, R., & Bersanelli, M. 1994, ApJS, 93, 125
Garilli, B., & Maccagni, D. 1990, A&A, 229, 88
Ghisellini, G., & Maraschi, L. 1989, ApJ, 340, 181
Ghisellini, G., Maraschi, L., & Treves, A. 1985, A&A, 146, 204
Ghisellini, G., Padovani, P., Celotti, A., & Maraschi, L. 1993, ApJ, 407, 65
Grandi, P., et al. 1994, Adv. Space Res. 15, 23
Impey, C. D., & Neugebauer, G. 1988, AJ, 95, 307
Keel, W. C. 1986, ApJ, 302, 296
Knapp, G. R., & Patten, B. M. 1991, AJ, 101, 1609
Lin, Y. C., et al. 1995, ApJ, 442, 96
Macchetto, F., et al. 1991, ApJ, 369, L55
Maraschi, L., Ghisellini, G., & Celotti, A. 1992, ApJ, 397, L5
Maraschi, L., et al. 1994a, ApJ, 435, L91
Maraschi, L., Ghisellini, G., & Celotti, A. 1994b, in IAU Symp. 159, Multiwavelength Continuum Emission of AGN, ed. T. J.-L. Courvoisier & A. Blecha (Dordrecht: Kluwer), 221
Maraschi, L., & Rovetti, F. 1994, ApJ, 436, 79
Orr, M. J. L., & Browne, I. W. A. 1982, MNRAS, 200, 1067
Pian, E., Falomo, R., Scarpa, R., & Treves, A. 1994, ApJ, 432, 547
Preston, R. A., et al. 1989, AJ, 98, 1
Punch, M., et al. 1992, Nature, 358, 477
Quinn, J., et al. 1995, IAU Circ., No. 6178
Sambruna, R. M., Barr, P., Giommi, P., Maraschi, L., Tagliaferri, G., & Treves, A. 1994, ApJ, 434, 468
Scarpa, R., Falomo, R., & Pian, E. 1995, A&A, in press
Shen, B. S. P., Usher, P. D., & Barrett, J. W. 1972, ApJ, 171, 457
Sikora, M., Begelman, M. C., & Rees, M. J. 1993, in Compton Gamma-Ray Observatory (AIP Conf. Proc. 280), ed. M. Friedlander, N. Gehrels, & D. J. Macomb (New York: AIP), 598
———. 1994, ApJ, 421, 153
Sparks, W. B., Biretta, J. A., & Macchetto, F. 1994, ApJS, 90, 909
Stecker, F. W., de Jager, O. C., & Salamon, M. H. 1992, ApJ, 390, L49
Stickel, M., Padovani, P., Urry, C. M., Fried, J. W., & Kühr, H. 1991, ApJ, 374, 431
Thompson, D. J., et al. 1994, in IAU Symp. 159, Multiwavelength Continuum Emission of AGN, ed. T. J.-L. Courvoisier & A. Blecha (Dordrecht: Kluwer), 49
Treves, A., Belloni, T., Falomo, R., Fink, H. H., Maraschi, L., Sambruna, R. M., Tagliaferri, G., & Zimmermann, H. U. 1993, ApJ, 406, 447
Ulrich, M. H., Hackney, K. R. H., Hackney, R. L., & Kondo, Y. 1984, ApJ, 276, 466
Unwin, S. C., Cohen, M. H., Biretta, J. A., Pearson, T. J., Seielstad, G. A., Walker, R. C., Simon, R. S., & Linfield, R. P. 1985, ApJ, 289, 109
Urry, C. M., & Reichert, G. 1988, *IUE* NASA Newsletter, 34, 96
Urry, C. M., & Shafer, R. A. 1984, ApJ, 280, 569
Valtaoja, E. 1994, in IAU Symp. 159, Multiwavelength Continuum Emission of AGN, ed. T. J.-L. Courvoisier & A. Blecha (Dordrecht: Kluwer), 145
Von Montigny, C., et al. 1995, ApJ, 440, 525
Worrall, D. M., & Wilkes, B. J. 1990, 360, 396